Abrupt grain boundary melting in ice

L. Benatov[1] and J. S. Wettlaufer[1,2]
[1]*Department of Physics, Yale University, New Haven, Connecticut 06520, USA*
[2]*Department of Geology and Geophysics, Yale University, New Haven, Connecticut 06520, USA*
(Received 14 August 2004; published 27 December 2004)

The effect of impurities on the grain boundary melting of ice is investigated through an extension of Derjaguin-Landau-Verwey-Overbeek theory, in which we include retarded potential effects in a calculation of the full frequency-dependent van der Waals and Coulombic interactions within a grain boundary. At high dopant concentrations, the classical solutal effect dominates the melting behavior. However, depending on the amount of impurity and the surface charge density, as temperature decreases, the attractive tail of the dispersion force interaction begins to compete effectively with the repulsive screened Coulomb interaction. This leads to a film-thickness/temperature curve that changes depending on the relative strengths of these interactions and exhibits a *decrease* in the film thickness with *increasing* impurity level. More striking is the fact that at very large film thicknesses, the repulsive Coulomb interaction can be effectively screened, leading to an abrupt reduction to zero film thickness.

DOI: 10.1103/PhysRevE.70.061606 PACS number(s): 68.08.Bc, 64.70.Dv, 92.40.Sn

I. INTRODUCTION

The original microscopic theories of melting focused on the criterion for the homogeneous breakdown of a harmonic solid lattice [1]. Elaborations of this perspective involve the thermal activation of defects or the instability of the lattice [2], but a theory of melting must treat bulk solid-liquid coexistence and recognize that solid matter in laboratory and natural conditions is finite and hence its bulk is disjoined from the surroundings by surfaces [1,2]. Hence, the melting of a *finite* crystal begins at one of its free surfaces at temperatures below the bulk transition [1]. This *interfacial premelting* occurs at the surfaces of solid rare gases, quantum solids, metals, semiconductors, and molecular solids and is characterized by the appearance of an interfacial thin film of liquid that grows in thickness as the bulk melting temperature, T_m, is approached from below. The relationship between the film thickness and the temperature depends on the nature of the interactions in the system. When interfacial premelting occurs at vapor surfaces, it is referred to as *surface melting*; when it occurs at the interface between a solid and a chemically inert substrate, it is called *interfacial melting*. When films at such solid surfaces diverge at the bulk transition, the melting is *complete*, but where retarded potential effects intervene and attenuate the intermolecular wetting forces, the film growth may be blocked and thereby be finite at the bulk transition. This latter circumstance, in which the behavior is discontinuous, is referred to as *incomplete* melting. The importance of grain boundary melting is great because of its potentially central influence on the sintering, coarsening, transport behavior, and many other bulk properties in ostensibly all materials. This fact has certainly not gone unrecognized, but nonetheless, the great difficulty of directly accessing a grain boundary in thermodynamic equilibrium has resulted in a dearth of experimental tests.

It is observed that, at temperatures below T_m, polycrystalline matter is threaded by the liquid phase driven solely by the impurity and curvature depressions of the freezing point (e.g., [3] for ice and [4] for metals). For example, the unfrozen water is found in microscopic channels, with a scale of $10-100\ \mu$m, called veins where three grains abut and at nodes separating four grains rather like the plateau borders in foams [3]. Hence, the equilibrium structure of polycrystalline ice is characterized by a connected network of water. Nye and Frank [5] predicted the geometry of the network under the assumption that the interfacial energies are independent of crystallographic orientation. In exact analogy with the classical force balance used to determine the contact angle of a partially wetting fluid on a substrate or the meniscus in capillary rise (e.g., [6]), their result considers the force balance at the trijunction where three grains come together. This provides an expression for the dihedral angle, $2\theta_0$, into which water intrudes, in terms of the simple ratio of the grain boundary, γ_{ss}, and solid-liquid, $\gamma_{s\ell}$, interfacial energies,

$$2\cos\theta_0 = \frac{\gamma_{ss}}{\gamma_{s\ell}}, \tag{1}$$

thereby determining the shape and cross section of a vein. Therefore, the concept of interfacial premelting and the vein-node network are related through grain boundary melting. Thus, during *complete* grain boundary melting, the dihedral angle vanishes and the single grain boundary is replaced by two interfaces: $\gamma_{ss} \rightarrow 2\gamma_{s\ell}$. This process is equivalent to the growth of a liquid film at the grain boundary and hence connects the dihedral angle, the vein/node/trijunction network, and grain boundary melting.

Because most materials exist in a polycrystalline state, their continuum properties, ranging from the mechanical and thermal properties of glaciers [3,5] to the reduction in the critical current density in high-temperature superconductors [7], are to a large extent controlled by the character of grain boundaries. However, although direct experimental probes of surface and interfacially melted films in thermodynamic equilibrium are common, experimental studies of grain boundary melting are centered on dihedral angle measurements. The disparity in the relevant length scales of grain

boundary films and the dihedral angle is such that while optical microscopy may be sufficient to determine the latter, the former requires a more highly resolved probe. Grain boundary melting poses serious experimental challenges because of the difficulty of direct access to the equilibrium interface of a bicrystal in a manner free of compromises associated with the proximity of surfaces associated with apparatus. Although computer simulations and theory support the notion of disorder at a grain boundary [8–11], experimentally it is often stimulated using impurities and then quenching a system before probing the boundary (e.g., [12,13]). Experiments in aluminum using electron microscopy have shown that as the temperature rises, the boundary structure remains epitaxial until $T=T_m$, when the grain boundary has the signature of bulk liquid [14]. Dihedral angle experiments on bismuth bicrystals placed in contact with the melt were performed for various crystallographic mismatches by Glicksman and colleagues (see [15] and references therein). They interpreted their data to indicate a discontinuous grain boundary melting transition as a function of grain mismatch. Relative to the abundant work on surface and interfacial melting, the present experimental edifice for grain boundary melting in all materials is lacking. From the standpoint of materials science, the advantage of studying ice is that the melting temperature is easily accessible in the laboratory without substantial cryogenics or heaters. Moreover, ice is transparent and birefringent and hence amenable to optical probing. Therefore, the dual importance of grain boundary melting in materials in general and in ice in particular make a compelling case for systematic measurements in ice. Ice provides the ideal test bed for such measurements and its propitious geophysical importance is a prime motivator [16]. The theory described here is intended to form a rostrum for experimental studies.

II. THEORY

A. Background

Complete interfacial melting is determined by the competition between bulk and surface free energies and requires that the total excess surface free energy per unit area, $F_{\text{total}}(d)$, be a positive monotonically decreasing function of the film thickness with a global minimum at infinite film thickness. In grain boundary melting $F_{\text{total}}(d)=\gamma_{ss}(d)$. It is conceptually useful to consider the thickness-dependent contributions to $\gamma_{ss}(d)$ to arise from ostensibly short- and long-ranged intermolecular interactions, namely wetting forces. Hence, we write the excess surface free energy as $\gamma_{ss}(d)=2\gamma_{s\ell}+F_{\text{short}}(d)+F_{\text{long}}(d)$, where as above $\gamma_{s\ell}$ is the interfacial free energy per unit area of the ice-water interfaces, with implicit reference to the crystallographic orientation present at an interface. Hence, by definition, at large enough distances, the long-range interactions always dominate over shorter-range interactions. Therefore, if interactions underlying $F_{\text{long}}(d)$ are attractive, that is, if they are represented by a negative monotonically increasing function of d, then $\gamma_{ss}(d)$ can never have a global minimum at $d=\infty$. However, if a short-range interaction $F_{\text{short}}(d)$ favored grain boundary melting, it may prevail over $F_{\text{long}}(d)$ out to large film thicknesses; $|F_{\text{short}}(d')|\geqslant|F_{\text{long}}(d')|$ for $0\leqslant d\leqslant d'$. The *magnitude* of the global minimum in $\gamma_{ss}(d)$ may then be quite small but will nonetheless occur at a large (but finite) value of $d\equiv d_{\text{min}}$, that is, $\gamma_{ss}(d_{\text{min}})\equiv\min[\gamma_{ss}(d)]\equiv\Gamma$. If this were the case, most physical observations of the system would be virtually indistinguishable from those expected for complete melting. A complete calculation of $\gamma_{ss}(d)$ allows one to estimate both the dihedral angle and the temperature at which the film thickness would saturate, each as a function of the thickness d_{min}. The dihedral angle θ_0 is given by $\cos\theta_0=1+(\Gamma/2\gamma_{s\ell})$, and hence, in the pure case, we estimate the temperature at which the film thickness saturates as given by $T-T_m\approx(T_m/\rho_s q_m)(\Gamma/d_{\text{min}})$, where ρ_s and q_m are the density and heat of fusion of ice. As we shall see, in the general case there is no strict separation of the thickness dependence of $\gamma_{ss}(d)$ because $F_{\text{short}}(d)$ can be quite long range, which makes the situation unique.

Our theoretical approach employs the full frequency-dependent dispersion (van der Waals) force contributions to the long-ranged interaction (e.g., [17,18]) and Poisson-Boltzmann theory for screened Coulomb interactions. The same basic physical phenomena form the basis of Derjaguin-Landau-Verwey-Overbeek (DLVO) theory [19–21]. The principal difference between this approach and the *modified* DLVO theory used previously to study surface and interfacial melting [22] is that the van der Waals interactions are calculated rigorously rather than using the phenomenological treatment of relevance in that case in which dispersion forces could be treated in the nonretarded limit.

There are two motivations for taking a more complex approach. First, when the *only interactions* in the system are nonretarded dispersion forces, or van der Waals forces, the total excess surface free energy per unit area is most commonly denoted by $F_{vdW}(d)=-A_H/12\ \pi\ d^2$, where A_H is the Hamaker constant (e.g., [20]). For identical substrates (e.g., ice/water/ice) separated by distance d, the Hamaker constant is positive, producing an attraction and consequently, as has been pointed out by other authors [10,23], grain boundary melting under dispersion forces must be incomplete. If, however, the substrates are separated by an electrolyte solution, they may be held at bay by repulsive screened Coulomb interactions. Second, for dissimilar materials, the van der Waals contribution can be both attractive and repulsive and one can observe oscillations in the force versus distance/film thickness curve leading to the possibility of the system being trapped in a local rather than global minimum [17,18,24,25]. Such is the case of the surface and interfacial melting of ice [17,18]. We do not expect this particular behavior in the case of the grain boundary under the influence of dispersion forces alone. However, when combined with repulsive screened Coulomb interactions, the effective interfacial free energy does indeed exhibit behavior that is analogous to the dispersion force contribution to the interfacial melting of ice. For example, as discussed in general terms above, depending on the electrolyte concentration, we can observe a global minimum at infinite, finite, or zero film thickness, but with a maximum at intermediate film thickness and a positive monotonically decreasing free energy at large film thickness.

These phenomena, in part associated with retardation, thereby heighten our appreciation of the importance of a quantitative treatment of the long-ranged forces in the system requiring a more complete calculation of $F_{vdW}(d)$.

The calculation of frequency-dependent dispersion force contributions to grain boundary melting are described in Sec. II C, but it is prudent to first remind ourselves of the general understanding of ice surfaces under the influence of such interactions. Generally speaking, when dispersion forces dominate, the wetting of *any* ice surface by water at temperatures below T_m will be facilitated when the polarizability of the water lies between that of the ice and the other material, be it a gaseous phase, a chemically inert solid, or ice. A particular novelty of the system, first pointed out by Elbaum and Schick [17] in their study of the surface melting of ice, is that the appropriately transformed polarizability of ice is greater than that of water at frequencies higher than approximately 2×10^{16} rad s^{-1}, whereas it is smaller at lower frequencies. Thus, so long as the surface melted layer of water is thin, the polarizabilities at all frequencies contribute additively to $F_{vdW}(d)$, whereas upon thickening, *retardation*—the attenuation of the interaction due to the finite speed of light—reduces the high-frequency contributions and favors those in which the polarizability of water dominates over that of the ice. Hence, with regard to the dispersion force contribution to the premelting of an ice surface, we expect the process to be complete when the third phase in the system possesses a low-frequency polarizability greater than that of water, and unattainable if the low-frequency polarizability is less than that of water. Many, if not most, solids have dielectric properties that lead to complete interfacial premelting, whereas the vapor phase of ice does not.

The great sensitivity of surface melting experiments to the presence of impurities led one of us [22] to introduce electrolytes into a model that did not include retardation. Here, as in that case, we consider the ions that underlie the repulsive screened Coulomb interactions in the canonical ensemble, and the entire ice/solution system is treated in the grand canonical ensemble [22]. Hence, because the ions are insoluble in the solid phase and the Debye length characterizing the range of the interactions is inversely proportional to the square root of the ion density, then the range and strength of this contribution to grain boundary melting is sensitive to the impurity level. Therefore, it is required that we properly capture the competition between repulsive screened Coulomb interactions and attractive dispersion forces at very long range, which is done through the use of Debye-Hückel theory in the appropriate ensemble and the complete theory of Dyzaloshinskii, Lifshitz, and Pitaevskii [27]. We now describe the various contributions to the excess surface energy in turn, the total free energy of the system, and the associated predictions.

B. Ionic force effects

The screening of surface charge is described by the Poisson-Boltzmann (PB) equation for the electrostatic potential ψ created by the distribution of ions of number density $n(z)$ throughout the film. For a monovalent electrolyte, and a surface potential ψ_s less than 25 mV, the Poisson-Boltzmann equation can be linearized in the Debye-Hückel limit, which yields

$$\psi(z) = \psi_s e^{-\kappa z}, \quad \text{where} \quad \kappa^{-1} = \left(\frac{\epsilon\epsilon_o k_b T}{e^2 n_b}\right)^{1/2} \tag{2}$$

is the Debye length, which captures the characteristic fall off of the ion field in the direction z normal to the surface. The bulk ion density is n_b, ϵ is the dielectric constant of the film, ϵ_o is the free space permittivity, e is the elementary charge, and k_bT is the usual thermal energy. The repulsive force between two charged surfaces originates in the restriction of the configurational entropy of the ions as the surfaces are brought closer. The resulting excess interfacial free energy per unit area across a film of thickness d is written

$$F_{DH}(d) \approx \frac{2q_s^{\,2}}{\kappa\epsilon\epsilon_o} e^{-\kappa d}, \tag{3}$$

where q_s is the surface charge density, discussed in more detail in Sec. II D. In the classical context of DLVO theory, the Debye length is a constant, and Eq. (3) can be considered in the same sense as $F_{\text{short}}(d)$ above. At this stage we simply note that it describes the electrostatic contribution to total excess interfacial free energy of relevance to the grain boundary melting of ice in the presence of electrolytes.

We point out several important modifications to PB theory beyond the obvious simplifications associated with the linearization, or weak-coupling limit (e.g., [28]), that led to Eq. (2). First, as a mean-field theory, ion-ion correlations and discrete ion-solvent interactions are not captured and the solvent is treated as a continuous medium [29]. Second, there are dispersion forces between ions and the surfaces that bound them, which can be of much longer range than Debye-Hückel theory would predict, although not of significant magnitude at a range beyond about 3 nm where retardation becomes important [21]. Such ion dispersion forces can influence the *static* van der Waals interactions in the system significantly for high dopant levels or multivalent ions [30]. Third, at molecular length scales, steric, or finite ion size, effects are important [31]. Although all of these phenomena may be of importance in a limited regime of the predictions presented here, we do not expect them to be responsible for a qualitative difference in the principal features described. Moreover, other equally distinct effects can also play a role. For example, in the case of the ion dispersion phenomena, the fact that the chemical potential of the ions in ice is effectively zero results in the film concentrating or diluting as a function of the departure from bulk coexistence, which leads to a film thickness dependence of the Debye length. Hence, we find a very-long-range repulsive interaction with an effectively algebraic structure. As for steric influences, at a grain boundary, other proximity effects associated with the crystallographic mismatch will be come equally important at short range. A theory that systematically includes all such effects on equal footing is still unwarranted by the state of

the experimental landscape, but we are compelled to note for the reader that we are acutely aware of all such complications and limitations enumerated in the detailed studies cited in this paragraph and in books on the topic [20,32].

C. Dispersion force effects

The frequency-dependent dispersion force, or van der Waals, contribution to the free energy of a surface consisting of a pure liquid water layer of thickness d between two slabs of bulk ice can be obtained from the theory of Dzyaloshinskii, Lifshitz, and Pitaevskii [27] (DLP). The result of this theory is an integral expression for the interfacial free energy per unit area, $F_{vdW}(d)$, in terms of the frequency-dependent dielectric polarizabilities of the ice (s) and the water (ℓ). In the sense described in Sec. II A, were grain boundary melting under dispersion forces alone to be considered, then $\gamma_{ss}(d)=2\gamma_{s\ell}+F_{\rm long}(d)\equiv 2\gamma_{s\ell}+F_{vdW}(d)$. Were complete grain boundary melting to be expected, and it is not, it would be indicated by a global minimum of $F_{vdW}(d)$ at $d\to\infty$ so that $\gamma_{ss}=2\gamma_{s\ell}$ at bulk coexistence. Incomplete grain boundary melting under dispersion forces is indicated by a minimum at finite d, with $F_{vdW}(d)$ negative there.

As described in Sec. II A, retarded potential effects are known to influence the qualitative nature of melting in ice. For example, the surface melting of ice has been observed to be incomplete due to retarded potential effects, whereas slight impurity doping leads to complete surface melting [17,26]. Because the neglect of retardation can lead to qualitatively and quantitatively different predictions, we append a brief discussion of the matter.

In order to make this development reasonably self contained, we present the DLP expression for $F_{vdW}(d)$ despite the fact that is has appeared in a variety of forms [17,18,24,27], and with sympathy to the girth of the literature we attempt the utmost brevity. The frequency-dependent dielectric response of the ice/water/ice system is described by

$$F_{vdW}(d)=\frac{kT}{8\pi d^2}\sum_{n=0}^{\infty'}\int_{r_n}^{\infty}dx\,x\left\{\ln\left[1-\left(\frac{x-x_s}{x+x_s}\right)^2e^{-x}\right]+\ln\left[1-\left(\frac{\epsilon_s x-\epsilon_\ell x_s}{\epsilon_s x+\epsilon_\ell x_s}\right)^2e^{-x}\right]\right\},\tag{4}$$

where

$$x_s=\left[x^2-r_n^2\left(1-\frac{\epsilon_s}{\epsilon_\ell}\right)\right]^{1/2},\tag{5}$$

and the material (s,ℓ) dielectric functions, corresponding to ice (ϵ_s) and water (ϵ_ℓ), are evaluated at the sequence of imaginary frequencies $i\xi_n=i(2\pi kT/\hbar)n$. The prime on the sum indicates that the $n=0$ term is weighted by $1/2$. The lower limit of integration is $r_n=2d(\epsilon_\ell)^{1/2}\xi_n/c$, and $k,\hbar$, and c have their usual meaning. The dielectric function required in the integral, $\epsilon(i\xi)$, is the analytic continuation of the material dielectric function $\epsilon(\omega)$ to imaginary frequencies. Lacking complete spectra for ice and water, as can be obtained in high melting temperature materials (e.g., [13]), we must generate the function by fitting the dielectric response of the material to a damped-oscillator model of the form

$$\epsilon(\omega)=1+\sum_j\frac{f_j}{e_j^2-i\hbar\omega g_j-(\hbar\omega)^2},\tag{6}$$

where e_j, f_j, and g_j are fitting parameters [33]. Each term in the sum corresponds to an absorption band of frequency, width, and oscillator strength, e_j, g_j, and f_j, respectively. Substitution of $i\xi$ for ω gives $\epsilon(i\xi)$, a well behaved, monotonically decreasing, real function of ξ.

We note that Eq. (4) assumes implicitly that ϵ_s is isotropic. Although the effect of the crystal orientation has been studied theoretically [34], no such polarization data were available for the present calculation. It has not been measured over the full frequency range, but judging from known values at optical frequencies [35], it is estimated to be small, and hence we neglect the small orientational dependence of the polarizabilities. Therefore, we treat the ice crystals as continuum dielectrics, with the surface crystal structure embodied by the surface charge density as described in Sec. II B.

D. Total free energy

The stable existence of an impure grain boundary film at temperatures below T_m is investigated by minimization of the total free energy of the system. The distinction between the canonical DLVO setting, say in colloid science, and surface, interfacial, or grain boundary melting is that in the former case the Debye length is constant for all values of the film thickness, whereas this is not the circumstance in the latter case [22]. We imagine doping a pure film with a monovalent electrolyte such as NaCl. Depending on the nature (low angle or twist) and magnitude of the mismatch between the crystals flanking the grain boundary, the solid-liquid interface will have a particular surface charge density q_s. We realize that each solid-liquid interface can, in principle, have a different value of q_s, and we embody the surface crystal structure through the surface charge density, but for the sake of simplicity and pedagogy we assume that both are equal. The surface charge is screened by the ions in the film, creating a repulsive interaction which competes with attractive long-ranged van der Waals interactions, and this embodies the excess surface energy.

We deposit N_i moles per unit area of a monovalent electrolyte in the grain boundary. The chemical potential of the electrolyte in ice is essentially zero [35], and because we are well below the solubility limit, the ions remain in the film with a concentration that is inversely proportional to film thickness. When the temperature decreases, the film thins, the ion concentration increases, and hence the Debye length decreases [see Eq. (2)]. At very low film thicknesses and very high ion concentrations, the limitations of PB theory, discussed in Sec. II B, come to the fore. Within these approximations, the behavior of the *total* free energy of the *system* determines the nature of grain boundary melting. For this we combine bulk and surface terms as

$$G_T(T,P,d,N_i) = \rho_\ell \mu_\ell(T,P)d + \mu_i(T,P)N_i + RTN_i \ln\frac{N_i}{\rho_\ell d} + \mu_s(T,P)N_s + \gamma_{ss}(d), \quad (7)$$

where $\gamma_{ss}(d) = 2\gamma_{s\ell} + F_{DH}(d) + F_{vdW}(d)$ is the total effective interfacial free energy combining Eqs. (3) and (4). The molar density, chemical potential per mole, and the number of moles per unit area of the solvent are ρ_ℓ, μ_ℓ, and $N_\ell = \rho_\ell d$, respectively, and the chemical potential of the impurity, the solid, and the number of moles of the latter are μ_i, μ_s, and N_s. We write the mixing entropy term, $RTN_i \ln(N_i/\rho_\ell d)$, where R is the gas constant, in the dilute limit of ideal solution theory, although we could simply replace the molar ratio by the activity coefficient for the impurity in the solvent. These complications do not change the principal regimes exhibited by the system.

The total free energy is minimized with respect to film thickness at fixed temperature and dopant concentration, and the integral in Eq. (4) and the dielectric fits for ice and water compiled from Ref. [36] were calculated in the same manner as was done previously [18,17]. The Gauss-Legendre quadrature integration scheme was tested against these calculations for the case of surface melting in the absence of impurities.

III. RESULTS

A representation of what we see overall as we vary the parameters is shown in the figure. In a given calculation, we ascribe a surface charge density to both solid/film interfaces, with, for example, $q_s = 0.01$ C m^{-2} corresponding to approximately four elementary charges per 1000 molecular sites. This particular case is rather high from the perspective of counting missing bonds at the interface or ionization defects, but conservative from the perspective of charge adsorption. It is useful to begin in the upper left-hand corner of Fig. 1(a) at high temperature. Consider the most dramatic curve first, namely the solid line which has the lowest dopant level of 6×10^{-5} μM m^{-2}. Due to the fact that in this case the Debye length is extremely long and the repulsive Coulomb interaction is longer ranged than the attractive van der Waals interaction, a very thick film of liquid exists at the ice grain boundary. As the temperature is lowered, the efficiency with which ice rejects electrolytes causes the film to be enriched with ions, and hence the Debye length, and the range of the Coulomb interaction, decreases until such point that the attractive tail of the van der Waals force begins to come into its own. As the temperature decreases, a point is reached where abruptly the van der Waals interaction dominates and drives a discontinous transition to zero film thickness. The transition moves to higher temperatures as the surface charge density and dopant levels decrease, thereby showing the expected behavior for melting driven solely by dispersion forces, that is, no grain boundary melting. An increase in the initial dopant level reduces the Debye length and the strength *and range* of the screened Coulomb interaction. Hence the plateau where the van der Waals and screened Coulomb interactions compete shifts to lower film thicknesses. If the

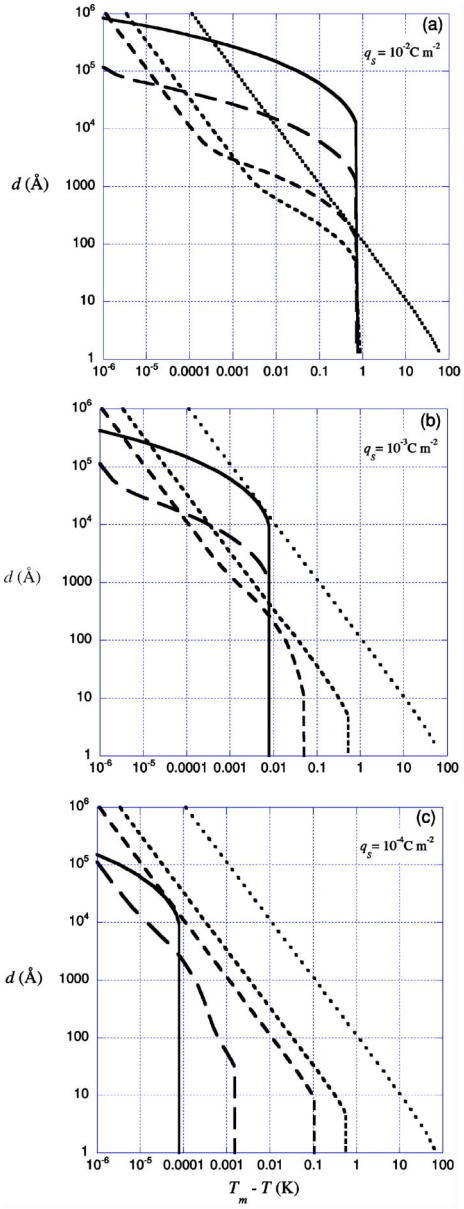

FIG. 1. Film thickness (Å) vs undercooling (Kelvin) for various monovalent electrolyte (NaCl) concentrations at an ice grain boundary with a solid/film surface charge density q_s of (a) 0.01 C m^{-2}, (b) 0.001 C m^{-2}, and (c) 0.0001 C m^{-2}. In (a)–(c), $N_i = 6\times10^{-5}$ (solid line), 6×10^{-4} (long dashed line), 6×10^{-3} (medium dashed line), 1.8×10^{-2} (small dashed line), and 6 (dotted line) μM m^{-2}. At the lower dopant levels where the Debye length is long, we observe an abrupt or discontinuous onset of grain boundary melting. The transition moves to higher temperatures as the surface charge density and dopant levels decrease, thereby showing the expected behavior for melting driven solely by dispersion forces. Note, for example in (a), that at $T_m - T = 0.01$ K, the film thickness is not a monotonically increasing function of ion concentration. Indeed, the film thickness *decreases* with increasing concentration *until* a threshold level is surpassed. Hence, there is a transition from melting dominated by dispersion and ionic force interactions to that dominated by the more commonly considered colligative effects. In (b) and (c), we see that for low surface-charge densities, the Coulomb interaction is weak, resulting in a much less pronounced plateau, or complete absence thereof, except for the lowest dopant concentrations.

temperature and/or the dopant level is sufficiently high, the bulk free energy dominates the total free energy and, as found previously [22], a surface version of Raoult's law is seen, $d \propto (T_m - T)^{-1}$. Finally, the largest dopant levels lead to the bulk free energy dominating through the entire range, and we predict a measurable film thickness in an easily accessible and controllable experimental range of temperature from 0 to $-10\,^{\circ}$C. Although this latter behavior was observed in studies of interfacial melting using atomic force microscopy [37], there exist no observations on ice grain boundaries. We emphasize that at fixed temperature, the film thickness is not a monotonically increasing function of ion concentration *until* a threshold level is surpassed. Thus, there is a transition from melting dominated by dispersion and ionic force interactions to that dominated by the more commonly considered colligative effects. An exploration of variations in dopant levels and surface charge density reveals the same qualitative behavior.

IV. DISCUSSION

One effect not considered in the current theoretical framework that warrants discussion is the possible dependence of $\gamma_{s\ell}$ on impurities adsorbed at the interface. The low solubility of electrolytes in ice leads to an enhanced interfacial adsorption and will modify the solid/film interfacial free energy, $\gamma_{s\ell}$, in a manner that depends on, among other things, the magnitude of the surface charge density and the bulk electrolyte concentration. A *decrease* in $\gamma_{s\ell}$ will *enhance* grain boundary melting relative to the pure case, were there not a similar decrease in the dry grain boundary energy. Although it is well known that an image charge effect leads to an *increase* in the liquid/vapor interfacial free energy with electrolyte concentration, there is no quantitative measure of the phenomenon at the solid/liquid interface wherein the intrinsic ionization defects in the solid phase are available to screen the adsorbed ions. Indeed, the great sensitivity of the surface melting of ice to impurities, in part responsible for the transition from incomplete to complete melting [26], is quite strikingly demonstrated in the calculations shown here. However, deconvolution of the precise dependencies of the constituents of the interfacial energies on N_i, the coupling to the ionic forces in the solution within the PB framework, and the additional influences of ion-ion correlations, ion-solvent and ion-dispersion interactions, and steric effects described above, is beyond the scope of experimental evidence.

As described above, there are two principal ways in which grain boundary melting can be observed: scrutiny of the dihedral angle subtended by a grain boundary groove, or direct probing of the liquid film thickness at the boundary as a function of temperature. In principle, the dramatic nature of our predictions and their thermodynamic accessibility render them amenable to an experimental search. In the experimental scenarios that we envisage, the grain boundary of a bicrystal is in contact with the bulk solution at a classical grain boundary groove and, hence, it is theoretically possible to examine both the dihedral angle *and* the grain boundary thickness. However, the ensemble operative in our predictions leads to a particularly impurity-sensitive film thickness dependence of the Debye length; Eq. (2) leads to $\kappa = c\sqrt{N_i/d}$, where $c = 7.237 \times 10^7$ m$^{1/2}$ mol$^{-1/2}$ is a constant. If however, contact of the grain boundary film with a bulk reservoir of ions allows compositional equilibration between the film and the bulk, then the Debye length will not be a function of the film thickness and some qualitative aspects of the predictions will differ. We expect compositional equilibration for the thickest films, but the presence of a substrate field in the case of the thinner films may not facilitate such homogenization. This question is the subject of ongoing work.

There are different methods that probe different aspects of premelted liquid water. For example, infrared spectroscopy averages the premelted liquid in a polycrystalline sample [38], introduction of a force microscope tip of another material provides an indirect probe [37,39], bright x-ray reflectivity discerns short-range structural properties [40], and optical methods (e.g., [26,41]) distinguish between liquid water and ice. Regardless of the approach, our calculations indicate the preference of systematic doping over attempts to prepare a completely clean system.

In summary, we have studied the effect of impurities on the grain boundary melting of ice using an extension of Derjaguin-Landau-Verwey-Overbeek theory, in which we include retarded potential effects in a calculation of the full frequency-dependent van der Waals and Coulombic interactions within a grain boundary. We find that, depending on the amount of impurity and the surface charge density, as temperature decreases, attractive dispersion force interactions effectively compete with repulsive screened Coulomb interactions producing grain boundary melting through a discontinuous transition. At sufficiently high dopant concentrations, the classical solutal effect dominates the melting behavior. The effect is within the scope of experimental accessibility.

ACKNOWLEDGMENTS

Conversations and criticism from J.G. Dash, J. Neufeld, A.W. Rempel, E. Thomson, and L.A. Wilen are greatly appreciated. We wish to acknowledge the support of the NSF-OPP9908945, the Bosack and Kruger Foundation, and Yale University.

APPENDIX: RETARDATION EFFECTS

The detailed quantitative effects of retardation mentioned in Sec. II A are placed in this appendix because grain boundary melting under dispersion forces alone is incomplete. Retardation has been clearly described previously (e.g., [17,18,24,33]) by considering a general ice/water/X interface in which X denotes a "substrate" which may be pure water vapor. In the limit that $\epsilon_\ell \approx \epsilon_s \approx \epsilon_X \approx 1$, one can approximate Eq. (4) as

$$F_{vdW}(d) \approx -\frac{kT}{8\pi d^2} \sum_{n=0}^{\infty\prime} \left(\frac{\epsilon_s - \epsilon_\ell}{\epsilon_s + \epsilon_\ell} \right) \left(\frac{\epsilon_X - \epsilon_\ell}{\epsilon_X + \epsilon_\ell} \right) (1 + r_n) e^{-r_n}. \tag{A1}$$

The term e^{-r_n}, due to retardation, acts as a high-frequency cutoff to the sum which is inversely proportional to d.

When the substrate is pure water vapor, ϵ_X may be taken

equal to 1. In this case, it is clear that were $\epsilon_s - \epsilon_\ell < 0$ at all frequencies, $F_{vdW}(d)$ would be a monotonically *increasing* function of d and the film would not grow. Conversely, if $\epsilon_s - \epsilon_\ell > 0$ at all frequencies, then $F_{vdW}(d)$ would be a monotonically *decreasing* function and the film thickness would diverge as the melting temperature is approached. Because $\epsilon_s - \epsilon_\ell$ changes sign at frequency ξ_c, the resulting melting behavior is intermediate between these cases. In particular, for sufficiently large d, where the sum is dominated by the low-frequency terms, surface melting is inhibited. When the substrate is a solid material with arbitrary dielectric properties, the results are more complicated. The function ϵ_X now depends on frequency ξ, and $\epsilon_\ell(i\xi) - \epsilon_X(i\xi)$ may change sign. For all of the materials studied previously [18], we observed that $\epsilon_X > \epsilon_{s,\ell}$ in the frequency range $\xi < \xi_c$. Hence we found that for d large enough ($\approx$30 Å) to allow retardation to come into play, $F_{vdW}(d)$ will be a positive monotonically decreasing function of d, implying that the necessary condition for complete interfacial melting to occur is fulfilled. To determine whether there is another, deeper, minimum in the free energy at small film thicknesses requires implemention of the full dispersion force calculation embodied in Eq. (4).

[1] J. G. Dash, Contemp. Phys. **43**, 427 (2002).

[2] V. Sorkin, E. Polturak, and J. Adler, Phys. Rev. B **68**, 174103 (2003).

[3] H. Mader, J. Glaciol. **38**, 333 (1992); **38**, 359 (1992); J. F. Nye, in *Physics and Chemistry of Ice*, edited by N. Maeno and T. Hondoh (Hokkaido University Press, Sapporo, 1992), pp. 200–205; A. W. Rempel, E. D. Waddington, J. S. Wettlaufer, and M. G. Worster, Nature (London) **411**, 568 (2001).

[4] C. S. Smith, Trans. Am. Inst. Min., Metall. Pet. Eng. **175**, 15 (1948).

[5] J. F. Nye and F. C. Frank, in *International Association of the Science of Hydrology, Publication No. 95* (Symposium at Cambridge 1969, Hydrology of Glaciers) (I.A.S.H., Cambridge, 1973), pp. 157–161.

[6] P. J.G. De Gennes, Rev. Mod. Phys. **57**, 827 (1985); M. Schick, in *Les Houches, Session XLVIII, 1988–Liquids at Interfaces*, edited by J. Charvolin, J. F. Joanny, and J. Zinn-Justin (Elsevier, Amsterdam, 1990), pp. 415–497; G. J. Merchant and J. B. Keller, Phys. Fluids A **4**, 477 (1992).

[7] J. R. Thompson, H. J. Kim, C. Cantoni, D. K. Christen, R. Feenstra, and D. T. Verebelyi, Phys. Rev. B **69**, 104509 (2004).

[8] R. Kikuchi and J. W. Cahn, Phys. Rev. B **21**, 1893 (1980).

[9] J. Q. Broughton and G. H. Gilmer, Phys. Rev. Lett. **56**, 2692 (1986).

[10] M. Schick and W. Shih, Phys. Rev. B **35**, 5030 (1987).

[11] A. E. Lobkovsky and J. A. Warren, Phys. Rev. E **63**, 051605 (2001); Physica D **164**, 202 (2002).

[12] J. Luo and Y.-M. Chiang, Acta Mater. **48**, 4501 (2000).

[13] R. W. French, J. Am. Ceram. Soc. **83**, 211 (2000).

[14] T. E. Hsieh and R. W. Balluffi, Acta Metall. **37**, 1637 (1989).

[15] C. L. Vold and M. E. Glicksman, in *The Nature and Behavior of Grain Boundaries*, edited by H. Hu (Plenum, New York, 1972), pp. 171–183.

[16] J. G. Dash, H.-Y. Fu, and J. S. Wettlaufer, Rep. Prog. Phys. **58**, 115 (1995).

[17] M. Elbaum and M. Schick, Phys. Rev. Lett. **66**, 1713 (1991).

[18] L. A. Wilen, J. S. Wettlaufer, M. Elbaum, and M. Schick, Phys. Rev. B **52**, 12426 (1995).

[19] The original work is in B. V. Derjaguin and L. Landau, Acta Physicochim. URSS **14**, 633 (1941); E. J. W. Verwey and J. Th. G. Overbeek, *Theory of the Stability of Lyophobic Colloids* (Elsevier, Amsterdam, 1948).

[20] J. N. Israelachvili *Intermolecular and Surface Forces* (Academic, New York, 1992).

[21] S. A. Edwards and D. R. M. Williams, Phys. Rev. Lett. **92**, 248303 (2004).

[22] J. S. Wettlaufer, Phys. Rev. Lett. **82**, 2516 (1999).

[23] R. Lipowsky, Phys. Rev. Lett. **57**, 2876 (1986).

[24] R. Bar-Ziv and S. A. Safran, Langmuir **9**, 2786 (1993).

[25] W. Fenzl, Europhys. Lett. **64**, 64 (2003).

[26] M. Elbaum, S. G. Lipson, and J. G. Dash, J. Cryst. Growth **129**, 491 (1993).

[27] I. E. Dzyaloshinskii, E. M. Lifshitz, and L. P. Pitaevskii, Adv. Phys. **10**, 165 (1961).

[28] R. R. Netz, Eur. Phys. J. E **5**, 557 (2001).

[29] Y. Burak and D. Andelman, Phys. Rev. E **62**, 5296 (2000); J. Chem. Phys. **114**, 3271 (2001).

[30] R. R. Netz, Eur. Phys. J. E **5**, 189 (2001).

[31] I. Borukhov, D. Andelman, and H. Orland, Phys. Rev. Lett. **79**, 435 (1997).

[32] J. Mahanty and B. W. Ninham *Dispersion Forces* (Academic, London, 1976).

[33] V. A. Parsegian, in *Physical Chemistry: Enriching Topics from Colloid and Surface Science*, edited by H. van Olphen and K. J. Mysels (Theorex, La Jolla, CA, 1975), p. 25.

[34] A. DalCorso and E. Tosatti, Phys. Rev. B **47**, 9742 (1993).

[35] P. V. Hobbs, *Ice Physics* (Clarendon, Oxford, 1974).

[36] L. D. Kislovskii, Opt. Spectrosc. **7**, 201 (1959); W. M. Irvine and J. B. Pollack, Icarus **8**, 324 (1968); J. M. Heller, Jr., R. N. Hamm, R. D. Birkhoff, and L. R. Painter, J. Chem. Phys. **60**, 3483 (1974); J. Daniels, Opt. Commun. **3**, 240 (1971).

[37] A. Doppenschmidt and H. J. Butt, Langmuir **16**, 6709 (2000).

[38] V. Sadtchenko and G. E. Ewing, J. Chem. Phys. **116**, 4686 (2002).

[39] B. Pittenger, S. C. Fain, Jr., M. J. Cochran, J. M. K. Donev, B. E. Robertson, A. Szuchmacher, and R. M. Overney, Phys. Rev. B **63**, 134102 (2001).

[40] H. Dosch, A. Lied, and J. H. Bilgram, Surf. Sci. **327**, 145 (1995); S. Engemann, H. Reichert, H. Dosch, J. H. Bilgram, V. Honkimäki, and A. Snigirev, Phys. Rev. Lett. **92**, 205701 (2004).

[41] D. Beaglehole and D. Nason, Surf. Sci. **96**, 357 (1980); Y. Furukawa, M. Yamamoto, and T. Kuroda, J. Cryst. Growth **82**, 665 (1987).